

## **UC Merced**

### **Proceedings of the Annual Meeting of the Cognitive Science Society**

#### **Title**

Wiring Cost Minimization: A Dominant Factor in the Evolution of Brain Networks across Five Species

#### **Permalink**

<https://escholarship.org/uc/item/188398mx>

#### **Journal**

Proceedings of the Annual Meeting of the Cognitive Science Society, 45(45)

#### **Authors**

Huang, Mingyi

Yu, Yuguo

#### **Publication Date**

2023

#### **Copyright Information**

This work is made available under the terms of a Creative Commons Attribution License, available at <https://creativecommons.org/licenses/by/4.0/>

Peer reviewed

# Wiring Cost Minimization: A Dominant Factor in the Evolution of Brain Networks across Five Species

Mingyi Huang (myhuang20@fudan.edu.cn) and Yuguo Yu (yuyuguo@fudan.edu.cn)

Research Institute of Intelligent and Complex Systems, State Key Laboratory of Medical Neurobiology, MOE Frontiers Center for Brain Science, Institute of Science and Technology for Brain-Inspired Intelligence, Fudan University, 220 Handan Road, SH 200433 CN

## Abstract

There is substantial evidence to suggest that brain circuits have evolved to be highly efficient and robust while consuming relatively minimal energy. These circuits possess unique structural and functional properties, such as sparsity, complexity, and small-world nature. Studies suggest that brain network development is shaped by a trade-off between minimal wiring cost and efficient communication. However, it is not entirely clear which factors are most influential, and to what extent each factor contributes to this development. Our examination of several potential underlying factors reveals that, with connectivity guaranteed by a fixed degree distribution, minimizing wiring cost has the greatest impact on network structure, compared to factors such as maximizing the clustering coefficient or coefficient of variation for wiring length distribution. While the cost-efficiency balance is capable of optimally reproducing brain networks in five different species without degree constraints, minimizing wiring cost remains the primary determinant.

**Keywords:** Brain Connectivity; Cost-Efficiency; Wiring Optimization

## Introduction

Neural connections are shaped by experience from a long history of evolution. Remarkably, simple connectivity patterns can improve the efficiency of learning rules, demonstrating how the brain can use anatomy to compensate for biological limitations in known synaptic plasticity mechanisms (Raman & O’Leary, 2021). With more detailed connectomics provided by experiments, we may further reveal how brain connections are formed by the requirements of effective learning and limitations of energy consumption.

Then, what are the major constraints driving brain network connections? Recent studies show that the wiring cost of the brain scales with the number of neurons and synapses, suggesting the brain has evolved to minimize this cost (Ahn, Jeong, & Kim, 2006). Neuroscientists have also noted at a very early stage that the localization of neuronal components seemed to “save circuits”, that is, minimize the cost of creating and maintaining neural connections (y Cajal, 2019). In fact, wiring minimization can lead to an optimal layout where most neurons are located close to their actual positions as addressed in an experiment with *C.elegans* connectome (Chen, Hall, & Chklovskii, 2006).

Moreover, the brain’s structural and functional networks may also evolve to be highly efficient, with a high degree of small-worldness, characterized by a balance between local clustering and global integration, suggesting that connectivity

efficiency is also an important principle of brain organization (Achard & Bullmore, 2007). Network modularity, or the degree to which the brain is composed of distinct, specialized modules, may also be a constraint on brain evolution. Studies have found that the modularity of the brain’s functional networks increases with brain size, suggesting that modularity is also an important principle of brain organization (Bullmore & Sporns, 2009). If we consider the cost-efficiency policy in brain network structure, two quite contradictory constraints are low wiring cost and high efficiency, characterized respectively by physical cost and functional value of the topology, for instance, fewer processing steps on average. By reconstructing biological neural networks, evidence is provided to support the hypothesis of trade-offs between multiple constraints of brain networks (Yuhan, Shengjun, Hilgetag, Changsong, & Olaf, 2013). From another perspective, researchers also tried to explore possible factors considering the wiring length distribution of the network. The corresponding principle of maximum entropy was brought up to depict connections of different lengths (Song, Zhou, & Li, 2021), which was distinguished in species.

It is acknowledged that multiple factors interact to shape the development of brain structural networks during evolution, thus it would be important to consider the contribution of each factor as well as the interplay of all these factors. Here, by reconstructing structures of biological neural networks with wiring optimization models in 5 species including *C.elegans*, *drosophila*, mouse, macaque, and human, we try to compare the influence of each possible factor that influences the development of a brain network structure, explore and discuss the possible trade-off between features that may lead to an “optimal” design of networks.

## Materials and Methods

### Data resources and modification

To reproduce the network structure of neural systems considering wiring cost, the ground truth connectivity matrix, 3-D coordinate or distance between each pair of nodes in the network are necessary data for reconstruction and validation.

We used connectivity and distance matrices of *drosophila*, mouse, macaque, and human in 3D scale, as provided in (Song et al., 2021). The network connectivity for ***drosophila*** brain is available online in the FlyCircuit 1.2 database

(<http://www.flycircuit.tw>) which includes 2106 connections among the 49 LPUs. Labeled with green fluorescent protein, single neurons were imaged at high resolution. **Mouse** brain template was reconstructed based on tract-tracing data, which contains 112 areas and 6542 connections, can be found on the Allen Institute Mouse Brain Connectivity Atlas (<http://connectivity.brain-map.org>). The network connectivity for template **macaque** brain was a recent version of the online CoCoMac database (<http://cocomac.g-node.org/main/index.php>), derived from literatures on tract-tracing experiments in macaque brain, which includes 103 cortical areas and 2518 connections using a more detailed parcellation of the motor regions (Yuhan et al., 2013). **Human** brain template is reconstructed from diffusion weighted magnetic resonance imaging, based on deterministic tractography algorithms (Betzel & Bassett, 2018) and includes 128 cortical areas and 4736 connections.

For **C.elegans** the network is reconstructed at neuronal scale, whereas the connections are measured among brain areas for the other species. Network connectivity data of *C.elegans* is provided by (Cook et al., 2019) and includes all 302 neurons and 5515 connections. The spatial layout of *C.elegans* neurons was rearranged into 3D coordinates (Fig.1C) by combining the 2D layout provided in (Yuhan et al., 2013) that contains 277 neurons and a 3D layout (Fig.1B) from Openworm (Sarma et al., 2018), a relatively detailed modeling work of nematodes. The 2D x-y coordinate for 277 neurons was kept since the 3D data exhibits a worm body with a sine curve. We first estimated the x-y position for 25 missing neurons and then aligned the third dimension coordinate to each node. The estimation was done by reconstructing a triangle for the missing neuron with the prepositions of 2 closest neighbors. The method was also tested within the 277 neurons, the error is overall around 2.5% compared to the mean distance between 2 nodes in the network, less than 0.95% the longest distance.

### Reconstructing Methods with constraints

**Generative Models** We tested two generative models to reconstruct the brain networks. For one we consider a degree restraint to reproduce null models with the same degree distribution as the real connection matrix, and then optimize the target feature with a convex optimization algorithm provided in Matlab as in Song et al. (2021).

In another method as applied in Yuhan et al. (2013), without demanding the same degree distribution, the feature is optimized by a simulated annealing algorithm with provided locations of nodes or distances between each pair of nodes. The simulated annealing started with a random network, an initial temperature  $T_0$  and then decreased temperature as  $T_{n+1} = T_n/n$ . At each temperature, the network is rewired for 1000 steps. At each step, we exchange the connections within four random nodes, and accept the changes with the probability  $\exp(-\Delta L/T)$ . The program is terminated when  $\Delta L \leq 10^{-6}$ .

Both methods are utilized to generate reconstructions that individually optimize a specific feature of the network to val-

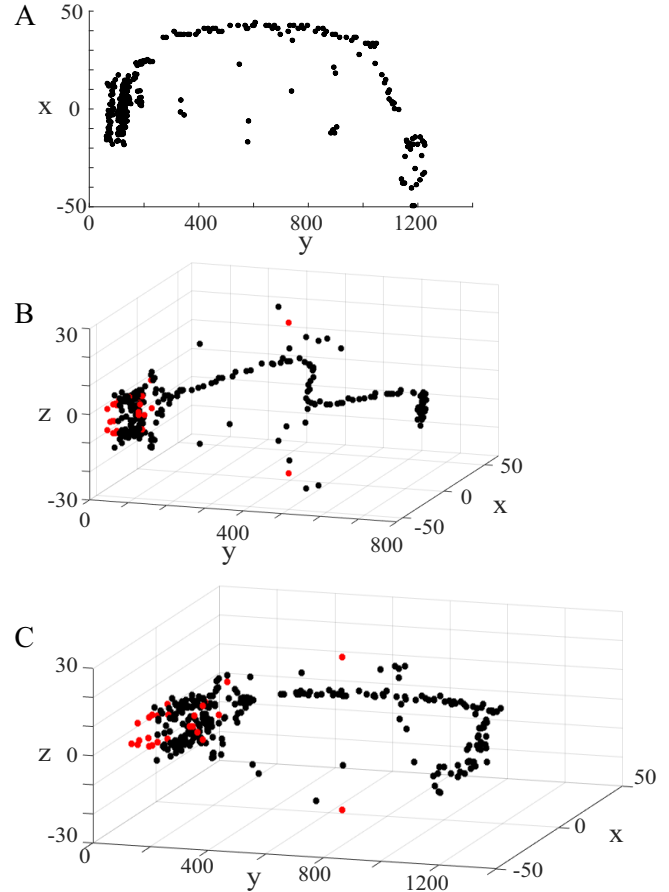


Figure 1: The spatial layout for neurons in *C.elegans* neural network. (A) 2D layout for 277 neurons. (B) 3D layout of 302 neurons with the sine-curved body. (C) Modified 3D layout of 302 neurons. Red dots represent the 25 neurons added in estimated x-y coordinates.

idate the impact of each feature.

**Complex network quantification indicators** We generated theoretically-optimized models for the constraints of features listed below.

**Modularity(Q)** is calculated as defined in Newman (2004):

$$Q = \frac{1}{K} \sum_{i,j} [A_{ij} - \frac{k_i k_j}{K}] \delta_{c_i c_j}$$

where,  $A_{ij} = 1$  when there is a projection between node  $i$  and node  $j$ , and 0, otherwise.  $K$  is the total number of links in this network,  $\delta$  is the Kronecker delta ( $\delta_{ij} = 1$  if  $i = j$ , and 0 otherwise), and  $c_i$  is the index of the community where node  $i$  is assigned. This measure quantifies the quality of the division of a network into modules or communities. High value indicates that the network has dense connections within communities and sparse connections between communities, which can be useful for understanding the organization of the network and identifying functional groups or clusters.

**Clustering coefficient(CC)** for a undirected network graph  $G = (V, E)$  is defined as Watts and Strogatz (1998):

$$C_i = \frac{2|\{e_{jk} : v_j, v_k \in N_i, e_{jk} \in E\}|}{k_i(k_i - 1)}$$

$$CC = \frac{1}{n} \sum_{i=1}^n C_i$$

where  $C_i$  is clustering coefficient of node  $v_i$  that measures the degree to which this node tends to be clustered into its neighborhood,  $N_i = \{v_j : e_{ij} \in E\}$  indicates its neighborhood and  $|\{e_{jk} : v_j, v_k \in N_i, e_{jk} \in E\}|$  is the number of connections between neighbors of  $v_i$ . The clustering coefficient suggests the local connectivity or cliquishness of the network. A high value indicates that the network has tightly connected local groups, where neighbors of a node are also connected to each other. This can be useful for understanding the resilience of the network to perturbations, as well as its potential for promoting redundancy, cooperation, or information-sharing among nodes. During the optimization, we calculate  $Q$  and  $CC$  with the BCT toolbox within Matlab.

**Total shortest path length( $L_g$ ) and total wiring length( $L_p$ )**, as two extreme points of a trade-off considered in Yuhan et al. (2013), were used to represent the effect of the processing efficiency and the physical cost respectively. For a specific network,  $L_g$  is the sum of the lowest step number between all pairs of nodes if one can reach another on the network graph, whose small value indicates a "small-world" property, where nodes can be reached quickly from other nodes, promoting efficient information flow or transportation. In contrast, a large average path length suggests a less efficient network in terms of information flow.  $L_p$  is the summation of the length of existing connections, assuming that the connections between nodes have an associated cost proportional to their length.

**Entropy( $H$ )** of a wiring length distribution, can be calculated by:

$$H = - \sum_{i=1}^k p_i \log(p_i)$$

where we categorize edges into  $k$  bins by order of wiring length, and  $p_i$  indicates the probability of a wiring length being in  $i^{th}$  bin. Entropy of wiring lengths in a complex network can provide insights into the diversity and distribution of connection distances between nodes. Higher values indicate a more diverse distribution of wiring lengths, suggesting that the network has a mix of short and long connections, while lower values imply a more uniform or predictable distribution of wiring lengths, indicating that the network has a more regular structure with connections of similar lengths.

**Coefficient of variation** for distribution over lengths of each connection ( $CV_l$ ) or degree of each node ( $CV_d$ ) is given by  $CV = \sigma/\mu$  where  $\sigma$  and  $\mu$  represent the standard deviation and mean value of the distributions respectively, suggesting a tradeoff between small physical cost and large structural diversity of the network considering wiring lengths distribution for  $CV_l$  or connection number of nodes for  $CV_d$ .

Among the factors addressed here, the modularity( $Q$ ), clustering coefficient( $CC$ ) and  $L_g$  can be used to depict information transmission efficiency of a network from different perspectives. The entropy of wiring length distribution ( $H$ ),  $CV_l$  and  $L_p$  can be particularly useful for studying spatial networks, where the nodes have specific spatial positions and the connections between nodes have associated physical distances or costs.

## Evaluation Methods

To quantify the difference between actual connectivity and reconstructed networks that are both binary, we calculate scores such as the recall rate or the recovery rate. As the recall rate only considers the correct predictions of existing connections, considering the brain network structures are usually sparse (much fewer 1 than 0 exists in the binary connection matrix), we choose the recovery rate calculated as in Yuhan et al. (2013). We use the calculation proposed in Costa, Kaiser, and Hilgetag (2007) to compute the recovery rate as  $R = \sqrt{R_0 R_1}$ .  $R_0 = K_{r1}/K_1$  and  $R_1 = K_{r0}/K_0$  are the recovery rate of 1 and 0, where  $K_{r1}$  and  $K_{r0}$  are the number of overlapping entries with value 1 and 0, respectively.

## Results

### Given degree distribution of real connectome, minimizing $L_p$ outweighs other individual feature optimizations

As addressed in Song et al. (2021), Brain connections become structurally diverse by maximizing entropy to support efficient inter-regional communication, providing potential organizational principles for brain networks. By using Shannon entropy to quantify the structural diversity of brain networks, researchers found that the distribution of wiring lengths across multiple species, including drosophila, mouse, macaque, human, and C.elegans, follows the principle of maximum entropy under constraints of limited wiring materials and spatial locations of brain regions or neurons. The generative model, under the strict restraint of the same degree distribution in real data, showed that for 5 species, the generated network exhibits high similarity with the real network.

We first replicate the results from a previous study using the original data provided (Song et al., 2021). The target function ( $F$ ) to be optimized was a combination of wiring length entropy  $H$  and total wiring length  $L_p$ :

$$F = H - \lambda L_p$$

where the coefficient  $\lambda$  is differently chosen for each species and can be actually understood as a trade-off between two features. We also apply the method to a modified 3D layout for C.elegans and found a recovery rate of less than 45.47% using 277 neurons.

Then, we evaluate the impact of the two factors individually by maximizing  $H$  and minimizing  $L_p$  separately and obtain higher or the same recovery rate with minimized  $L_p$

for all 5 species compared to the original generative model that combines minimizing cost with the principle of maximum entropy (Table.1). The recovery rate grows along with a growing portion of total wiring length ( $L_p$ ) in optimizing function.

Table 1: Recovery rate with degree constraint.

Species	Max $H$	Song et al. (2021)	Min $L_p$
C.elegans	35.27%	30.34%	47.46%
Drosophila	62.55%	69.71%	69.71%
Mouse	58.35%	63.76%	64.11%
Macaque	59.12%	70.36%	71.48%
Human	56.36%	73.85%	74.14%

We also reproduce the network structure by optimizing other features while maintaining the same degree of distribution as the real connectivity. Despite being constrained by the given degree distribution, we find that minimizing the total wiring length,  $L_p$ , is overall more effective than other features in reproducing the network structures of all five species (Fig. 2), despite the fact that maximizing the clustering coefficient was more effective in reproducing the drosophila brain.

Maximizing the coefficient of variation (CV) of wiring length distribution can also reproduces the brain structures well. Besides, maximizing modularity or minimizing the total shortest path length produced similar results as maximizing entropy, and the clustering coefficient produced a mildly improved reconstruction.

Table 1 shows that minimizing wiring length ( $L_p$ ) under the given network degree distribution resulted in the most accurate reproduction of brain network structures among the five species studied. This indicates that complex-network features related to degree distribution, along with wiring cost, play a crucial role as a trade-off.

Thus, as the connection degree is fixed, the total wiring length is minimized due to the higher energy cost of remote connections. This aligns with the idea of the Wiring Optimization principle, that nature favors layouts with minimal wiring length given a fixed pattern of connections (Chklovskii & Koulakov, 2004). In order to minimize the cost, brain circuits will develop in a way that optimizes the spatial connectivity of connections between neurons or brain components (Chklovskii & Stevens, 1999).

**Without the constraint of the actual degree distribution, the cost-efficiency trade-off leads to optimal reconstruction.** In the section above, we fix the degree distribution as in the real brain network, which assures connectivity while reconstructing the network structure. Thus, we further compare the factors without this precondition by generating random networks and optimizing each factor with a simulated annealing algorithm as in Yuhan et al. (2013).

Without fixing the degree distribution, the reconstruction accuracy is not as high as in Table 1, but we still observe

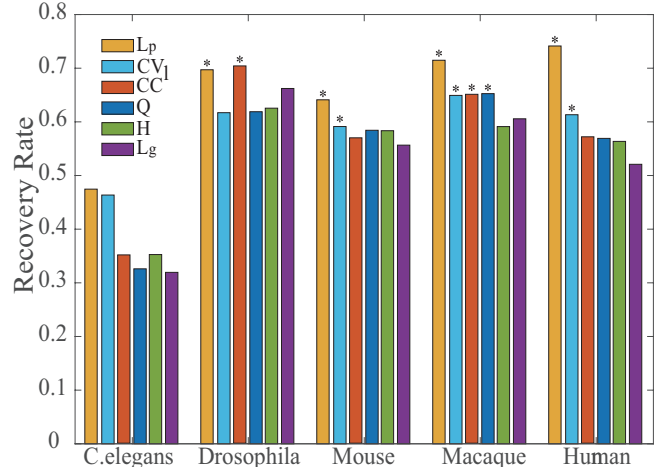


Figure 2: Recovery rate of connectivity matrix generated by single factor optimization. The overall performance of each factor is calculated as the mean recovery rate in 5 species and decays by order: total wiring length ( $L_p$  : 0.6538), coefficient of variation ( $CV_I$  : 0.5869) of wiring length distribution, clustering coefficient ( $CC$  : 0.5689), modularity ( $Q$  : 0.5502), entropy ( $H$  : 0.5433) of wiring length distribution and total shortest path length( $L_g$  : 0.5330). \* Tagged models are significantly better than null model.

that minimizing total wiring length  $L_p$  resulted in significantly higher recovery rates than minimizing total shortest path length  $L_g$ . The cost-efficiency trade-off is also reproduced as in Yuhan et al. (2013), an objective function combining the wiring cost and processing efficiency constraints:

$$L = (1 - \alpha)L_g^* + \alpha L_p^*$$

where the  $L_g^*$  and  $L_p^*$  are normalized by largest  $L_g$  and  $L_p$ . And we attain the best recovery rate when  $\alpha$  is close to 1 for all 5 species, which means the trade-off has a distinct bias toward wiring cost.

Table 2: Recovery rate without degree constraint with simulated annealing algorithm (Yuhan et al., 2013).

Species	Min $L_p$	Min $L_g$	Trade-off
C.elegans	43.41%	31.68%	46.13% ( $\alpha = 0.8$ )
Drosophila	74.12%	40.84%	74.12% ( $\alpha = 1$ )
Mouse	60.54%	34.16%	60.92% ( $\alpha = 0.8$ )
Macaque	63.28%	51.18%	63.62% ( $\alpha = 0.6$ )
Human	69.72%	39.86%	69.81% ( $\alpha = 0.8$ )

To further analyze the two constraints, we compare the reconstructed networks illustratively (Fig.3). The connectivity with minimizing  $L_p$  shows more modular structures while minimizing  $L_g$  does not.

Besides minimizing  $L_p$  and  $L_g$ , we also test maximizing maximizing Entropy ( $H$ ), the coefficient of variation of de-

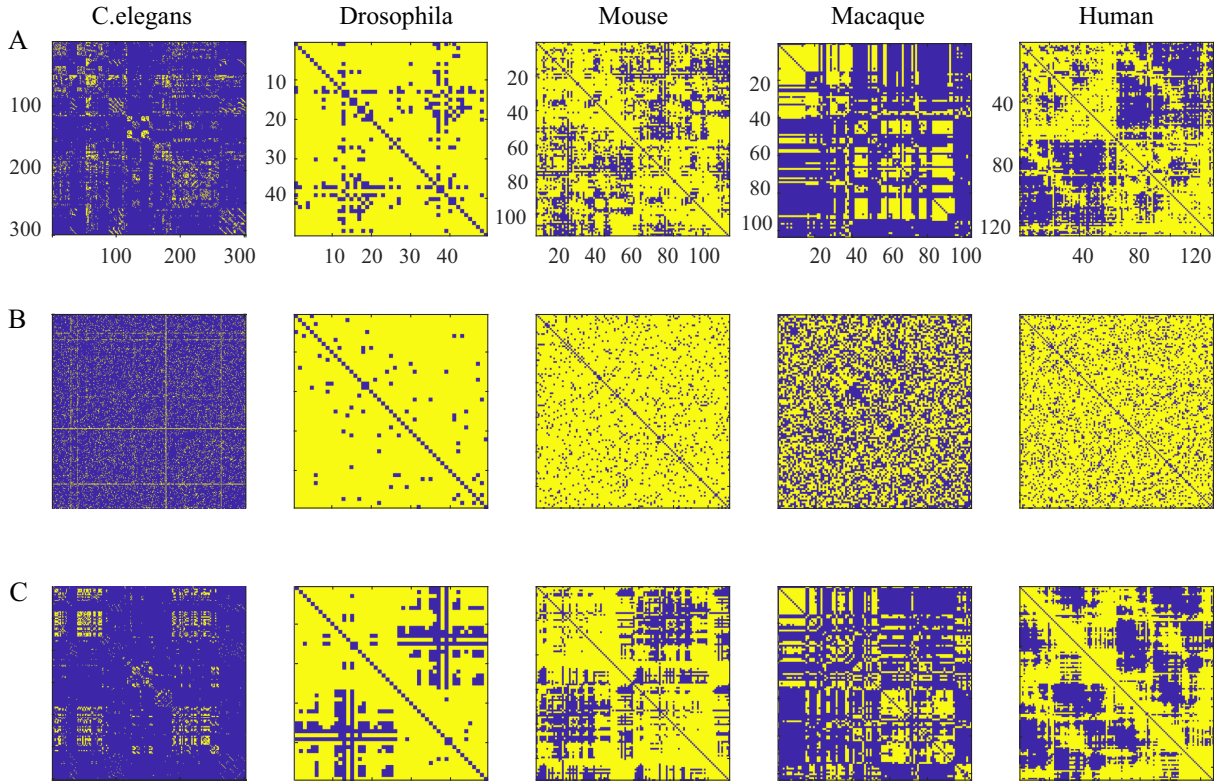


Figure 3: The reconstruction of neural networks in 5 species. Illustration of (A) real connectivity and connectivity reproduced by (B) minimizing  $L_g$  and (c) minimizing  $L_p$ .

gree distribution ( $CV_d$ ) and wiring length distribution ( $CV_l$ ) for celegans, drosophila, mouse, macaque and human data. Though not as influential as  $L_p$ , maximizing  $CV_l$  is still a more important factor comparing with maximizing  $CV_d$  or  $H$  in reconstruction (Table 3).

Table 3: Recovery rate for maximizing  $CV_d$ ,  $CV_l$  and  $H$ .

Species	Max $CV_l$	Max $CV_d$	Max $H$
C.elegans	47.15%	27.90%	29.27%
Drosophila	51.01%	64.38%	42.35%
Mouse	56.60%	44.24%	38.81%
Macaque	62.26%	45.72%	49.67%
Human	61.52%	53.00%	43.38%

We then compare differences in modularity ( $Q$ ), clustering coefficient ( $CC$ ), and the small-world characteristic ( $CC/L_g$ ) between real connectivity and theoretical reproductions. For each feature  $f$ , we estimate it for model network  $f_m$  and real network structure  $f_r$ , then the difference is given by  $E = (f_m - f_r)/f_r$  in Figure 4.

With minimum  $L_g$ , the reconstructed network derives less modular structure than the actual network. In contrast, for minimum  $L_p$ , the reconstructed one has overall higher  $Q$  than real connectome, especially for drosophila (Fig.4). By min-

imizing  $L_p$  with C.elegans spatial layout, a larger clustering coefficient but less degree of small-worldness is derived, indicating a much larger total shortest path length than real connectome. Reconstructions of maximizing  $CV_d$  and  $CV_l$  in 4 species show similar features to the actual networks except that maximizing  $CV_d$  or  $H$  also derives little modular structure as minimizing  $L_g$ .

## Discussion

Our study demonstrates that when utilizing the given degree distribution of real connectome, minimizing total wiring length resulted in the highest recovery rate among the single target optimization models tested in all five species. This suggests that when network connectivity is fixed, minimizing link costs serves as a trade-off between cost and communication efficiency. Therefore, it may not be necessary to consider an additional optimal compromise between entropy and link costs as previously proposed in Song et al. (2021).

When the degree distribution constraint is removed, we evaluated the trade-off between efficiency and cost by optimizing the wiring individually and as a combination. Although minimizing wiring cost had a greater impact on reconstructing the network structures, the optimal balance between connectivity efficiency and cost was still crucial in achieving maximum similarity between the reconstructed and real networks. This highlights that the brain's network seeks to

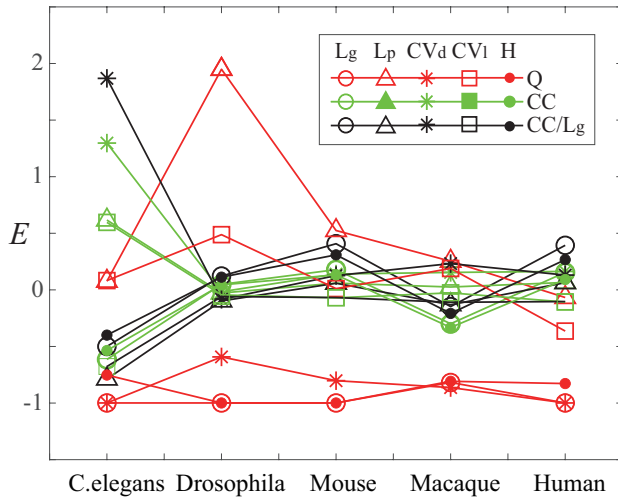


Figure 4: The difference of features between real and reconstructed neural networks. Circles stand for the reconstruction of  $\text{Min}(L_g)$ , triangles for  $\text{Min}(L_p)$ , stars for  $\text{Max}(CV_d)$ , squares for  $\text{Max}(CV_l)$ , and points for  $\text{Max}(H)$ . The difference of feature  $f$  between model network  $f_m$  and real network structure  $f_r$  is calculated by  $E = (f_m - f_r)/f_r$ . Different features are suggested by colors as in the legend.

achieve its complex functions with limited energy consumption through large connectivity and high communication efficiency.

Optimized neuroanatomy, as demonstrated in examples such as (Cherniak, Mokhtarzada, & Nodelman, 2002), shows that the most complex biological structures can arise from simple physical energy minimization processes. While wiring cost does play a significant role in determining the structure of neural systems, it is simply a constraint imposed by the limitations of energy and resources. It is widely acknowledged that the cost of wiring brain connections comes from factors such as volume, metabolic demands, signal delays and attenuation, and guidance defects during development (Chklovskii & Koulakov, 2004). However, to achieve an optimal structure that balances efficiency and function, a network must also meet other requirements. Recent research has highlighted the importance of characteristics such as a modular structure and widely distributed hubs (Bertolero, Yeo, Bassett, & D’Esposito, 2018), small wiring cost, and high efficiency within each hemisphere with minimal connections between hemispheres (Assaf, Bouznach, Zomet, Marom, & Yovel, 2020).

We believe a relatively optimized brain network should attain higher robustness and efficiency for flexible functions while keeping costs low in real brains. To achieve this, the brain network should possess features such as a flexible connection topology, efficient information transmission, and minimal wiring costs. Flexibility in the network allows for multiple pathways between nodes, ensuring robustness in in-

formation transmission. The presence of short paths or small-world properties characterizes efficient information transmission. However, it is important to note that there is a trade-off between minimizing costs and maximizing robustness or efficiency. For example, while long-distance connections may not greatly reduce path length, they can add diversity to brain area inputs and outputs, resulting in more complex brain dynamics (Betzel & Bassett, 2018). Therefore, minimizing wiring length should not be the ultimate goal during network formation, but rather a constraint to be considered in conjunction with other factors. In other words, neural networks tend to balance the trade-off between efficiency and robustness while being constrained by the cost of wiring.

## Acknowledgments

We are grateful for the support from the Science and Technology Innovation 2030-Brain Science and Brain-Inspired Intelligence Project (2021ZD0201301), the National Natural Science Foundation of China (U20A20221), the Shanghai Municipal Science and Technology Major Project (2018SHZDZX01 and 2021SHZDZX0103) and the ZJLab, Shanghai Municipal Science and Technology Committee of Shanghai Outstanding Academic Leaders plan (21XD1400400).

## References

- Achard, S., & Bullmore, E. (2007). Efficiency and cost of economical brain functional networks. *PLoS Comput Biol*, 3(2), e17.
- Ahn, Y. Y., Jeong, H., & Kim, B. J. (2006). Wiring cost in the organization of a biological neuronal network. *Physica A: Statistical Mechanics and its Applications*, 367, 531-537.
- Assaf, Y., Bouznach, A., Zomet, O., Marom, A., & Yovel, Y. (2020). Conservation of brain connectivity and wiring across the mammalian class. *Nat Neurosci*, 23(7), 805-808.
- Bertolero, M. A., Yeo, B. T. T., Bassett, D. S., & D’Esposito, M. (2018). A mechanistic model of connector hubs, modularity and cognition. *Nat Hum Behav*, 2(10), 765-777.
- Betzel, R. F., & Bassett, D. S. (2018). Specificity and robustness of long-distance connections in weighted, inter-areal connectomes. *Proceedings of the National Academy of Sciences*, 115(21), E4880-E4889.
- Bullmore, E., & Sporns, O. (2009). Complex brain networks: Graph theoretical analysis of structural and functional systems (nature reviews neuroscience (2009) 10, (186-198)). *Nature reviews Neuroscience*, 10, 186-198.
- Chen, B. L., Hall, D. H., & Chklovskii, D. B. (2006). Wiring optimization can relate neuronal structure and function. *Proc Natl Acad Sci U S A*, 103(12), 4723-8.
- Cherniak, C., Mokhtarzada, Z., & Nodelman, U. (2002). Optimal-wiring models of neuroanatomy. In G. A. Ascoli (Ed.), *Computational neuroanatomy: Principles and methods* (pp. 71-82). Totowa, NJ: Humana Press.
- Chklovskii, D., & Koulakov, A. A. (2004). Maps in the brain: what can we learn from them? *Annu Rev Neurosci*, 27, 369-92.

- Chklovskii, D., & Stevens, C. (1999). Wiring optimization in the brain. In S. Solla, T. Leen, & K. Muller (Eds.), *Advances in neural information processing systems* (Vol. 12). MIT Press.
- Cook, S. J., Jarrell, T. A., Brittin, C. A., Wang, Y., Bloniarz, A. E., Yakovlev, M. A., . . . Emmons, S. W. (2019). Whole-animal connectomes of both *caenorhabditis elegans* sexes. *Nature*, *571*(7763), 63-71.
- Costa, L. D. F., Kaiser, M., & Hilgetag, C. C. (2007, 02). Predicting the connectivity of primate cortical networks from topological and spatial node properties. *BMC systems biology*, *1*, 16.
- Newman, M. (2004, 07). Fast algorithm for detecting community structure in networks. *phys. rev. e stat. nonlin. soft. matter. phys.* *69*(6 pt 2), 066133. *Physical review. E, Statistical, nonlinear, and soft matter physics*, *69*, 066133.
- Raman, D. V., & O'Leary, T. (2021). Frozen algorithms: how the brain's wiring facilitates learning. *Curr Opin Neurobiol*, *67*, 207-214.
- Sarma, G. P., Lee, C. W., Portegys, T., Ghayoomie, V., Jacobs, T., Alicea, B., . . . Larson, S. D. (2018). Openworm: overview and recent advances in integrative biological simulation of *caenorhabditis elegans*. *Philos Trans R Soc Lond B Biol Sci*, *373*(1758).
- Song, Y., Zhou, D., & Li, S. (2021). Maximum entropy principle underlies wiring length distribution in brain networks. *Cereb Cortex*, *31*(10), 4628-4641.
- Watts, D. J., & Strogatz, S. H. (1998). Collective dynamics of 'small-world' networks. *Nature*, *393*(6684), 440-442.
- y Cajal, S. R. (2019). Textura del sistema nervioso del hombre y de los vertebrados, 1899–1904. In *Stripped bare: The art of animal anatomy* (pp. 216–219). Princeton: Princeton University Press.
- Yuhan, C., Shengjun, W., Hilgetag, C. C., Changsong, Z., & Olaf, S. (2013). Trade-off between multiple constraints enables simultaneous formation of modules and hubs in neural systems. *PLoS Comput Biol*, *9*(3), e1002937.